Underlay Cognitive Radio: What Is the Impact of Carrier Aggregation and Relaying on Throughput?

Panagiotis D. Diamantoulakis*, Koralia N. Pappi*, Sami Muhaidat†‡, George K. Karagiannidis*, and Tamer Khattab§
*Department of Electrical and Computer Engineering, Aristotle University of Thessaloniki, GR-54124 Thessaloniki, Greece
†Department of Electrical and Computer Engineering, Khalifa University, PO Box 127788, Abu Dhabi, UAE
‡Centre for Communication Systems Research (CCSR) - University of Surrey, Surrey GU2 7XH, UK
§Electrical Engineering, Qatar University, Doha, Qatar
e-mails: {padiaman,kpappi}@auth.gr, sami.muhaidat@kustar.ac.ae, geokarag@ieee.org, tkhattab@qu.edu.qa

Abstract—**In this paper, we investigate joint relay selection and optimal power allocation, as a means to maximize the achievable rate of an underlay cooperative cognitive radio with carrier aggregation, taking into account the availability of multiple carrier components in two different bands and primary users (PUs) with specific average outage probability requirements. For the acquisition of the interference thresholds, which are set by the PUs on the secondary user (SU), we incorporate a minimum feedback strategy into the problem formulation, based on the minimization of the PUs outage probabilities. The resulting non-convex optimization problem is transformed into a convex one and optimally solved using dual decomposition and an efficient iterative method with closed-form power policies. Simulation results illustrate that the proposed configuration exploits the available degrees of freedom in an efficient way which maximizes the SU throughput while the average outage probability of the PUs is kept at acceptable levels.**

I. Introduction

Cognitive Radio (CR) is a novel intelligent technique, which improves the utilization of the limited spectral resources, by identifying underutilized spectrum bands of the licensed (primary) users (PUs) [1]. Secondary users (SUs) are allowed to use frequency bands, which are already assigned to a PU, provided that they guarantee their Quality of Service (QoS) [2], [3]. The available spectrum for the SU transmission is usually dispersed, while the spectral usage of a SU may extend among different or heterogeneous networks [4]. Therefore, a secondary cognitive radio user may transmit and receive over multiple dispersed bands.

A key technology, which enables the usage of multiple spectrum segments aiming to provide substantially higher data rates and improved energy efficiency, is Carrier Aggregation (CA). CA is included in the 3GPP LTE-Advanced (LTE-A) standard [5] and it allows the aggregation of a maximum bandwidth of 100 MHz. It can aggregate component carriers (CCs) which belong to either the same band or different carrier bands. Thus, the combined spectrum may present diverse propagation characteristics, where communication in aggregated high frequency bands experiences high attenuation and path loss. In such cases, relays are used not only for diversity [6], [7], but also for coverage extension [8], [9].

The work of P. D. Diamantoulakis, G. K. Karagiannidis, and T. Khattab was funded by the NPRP grant # NPRP 6-1326-2-532 from the Qatar National Research Fund (a member of Qatar Foundation). The statements made herein are solely the responsibility of the authors.

Relay selection in CR has been investigated in [10]. However, joint relay selection and dynamic power allocation in underlay cognitive networks are considered only by sporadic works. In [11], the authors aim to maximize the total throughput, when only two data streams are sent over orthogonal frequencies, through the direct and a two-hop Amplify-and-Forward (AF) link. However, the provided solution cannot be directly extended to the case of CA which enables the utilization of multiple CCs and, thus, power allocation at the relay is required. A similar system model and optimization model is examined in [12], [13], where AF relaying is also considered, but multiple links instead of only one are now employed. However, the authors resort to oversimplified sub-optimal solutions based on equivalent noise minimization over each link. Moreover, the interference imposed by the PU is considered to be perfectly known and canceled at the SU, which increases the complexity of the decoding process and creates implementation difficulties. Most of the assumptions made in [12], [13] do not match the principles of underlay cognitive networks and CA. Furthermore, the aforementioned works in [11]–[13] assume perfect channel state information for the links between PU-SU, which is not realistic to acquire in practice.

Unlike recent literature, we consider the application of CA in an underlay cognitive radio network with relay selection, as a means to increase the achievable rate without causing harmful interference to the PUs. To this end, we address the aforementioned issues when the communication network is set as follows: i) the secondary source (S) sends multiple data streams to the secondary destination (D), aggregating CCs in two different frequency bands and performing underlay transmission, and ii) in the low frequency band, S and D communicate through a direct link, while in the high frequency band, they communicate via a two-hop relaying link. Furthermore, we formulate a joint power allocation and relay selection optimization problem, appropriate for throughput efficient communication in relay-assisted CA systems. Beyond this, the contribution of this work can be summarized as follows:

- A system formulation is assumed, which accommodates the existence of not only direct links between the source and the destination of the SU, but also the existence of two-hop AF relaying links for higher frequency carriers, where direct transmission is not feasible.

- A minimum feedback by the PUs towards the SU is considered, based on the minimization of the PUs outage probabilities.
- The formulated power allocation problem is transformed into a convex one and optimally solved by an efficient iterative algorithm. For this purpose, convex optimization tools and dual decomposition are applied. Also, a redundancy of relays is assumed for relay selection.
- Extensive simulation results show that the application of CA in cognitive networks, with proper joint power allocation and relay selection, can exploit the available bandwidth and boost the rate that the SU achieves.

II. System Model

An underlay SU network that employs CA is considered, aggregating CCs from a low frequency band ($l = 1$) and a high frequency band ($l = 2$), in order to achieve higher rates. One licensed PU, consisting of a transmitter T_{li} and a receiver V_{li}, operates over the i^{th} CC of the l^{th} band. The codebooks of all nodes are considered to be long zero mean unit variance complex Gaussian. Each channel coefficient between any two nodes, e.g. J and Q, follows a complex Gaussian distribution, i.e. $h_{jq|li} \sim \mathcal{CN}(0, 1/L_{jq|li})$ where $l = 1, 2$ and $i = 1, \ldots, N_l$, while the additive noise at node Q follows a complex Gaussian distribution with $n_{q|li} \sim \mathcal{CN}(0, W_{li}N_0)$. The notation used in the paper is summarized in Table I.

A. Primary Users Communication

Each T_{li} transmits a codeword z_{li} towards V_{li} over the i^{th} CC in the l^{th} band. The received signal at V_{li} is

$$y_{v|li} = \sqrt{P_{t|li}} h_{tv|li} z_{li} + I_{SU|li} + n_{v|li}. \tag{1}$$

B. Secondary User Communication

The SU utilizes the direct link $S \rightarrow D$ for the lower frequency band. Over the higher frequency band ($l = 2$), due to high path loss, we assume that there is no line-of-sight (LoS), thus the SU utilizes an AF half-duplex relay, selected out of M available relays (R_r, $r = 1, \ldots, M$). Communication between S and D is divided into two time-slots. In the first time-slot, S transmits over both frequency bands, and all relays receive over the high frequency band, while D receives over the low frequency band. In the second time-slot, S transmits only over the low frequency band while the selected relay transmits over the high frequency band, and D receives through all bands. The channel coefficients are considered constant over the two consecutive time-slots.

1) Direct Link over the 1^{st} *Band:* The transmission from T_{1i} is causing interference in the i^{th} CC. Thus the received signal at D is given by

$$y_{d|1i} = \sqrt{P_{s|1i}} h_{sd|1i} x_{1i} + \sqrt{P_{t|1i}} h_{td|1i} z_{1i} + n_{d|1i}, \tag{2}$$

where x_{1i} is the transmitted symbol. The received signal-to-interference-plus-noise-ratio (SINR) at D for the i^{th} CC is

$$\gamma_{1i} = \frac{P_{s|1i}|h_{sd|1i}|^2}{P_{t|1i}|h_{td|1i}|^2 + W_{1i}N_0}. \tag{3}$$

If $P'_{s|li}$ is the allocated power during the second time-slot instead of $P_{s|li}$, the corresponding SINR is denoted by γ'_{1i}.

2) Relay-Assisted Link over the 2^{nd} *Band:* In the first time-slot, S transmits data symbols over each CC of the 2^{nd} band towards the relays. Furthermore, transmission from each T_{2i} is causing interference during both time-slots. Thus, the received signal at the r^{th} relay node over the i^{th} CC is

$$y_{r|2i} = \sqrt{P_{s|2i}} h_{sr|2i} x_2 + \sqrt{P_{t|2i}} h_{tr|2i} z_{2i} + n_{r|2i}. \tag{4}$$

In the second time-slot, each relay - if selected - normalizes its received signal over the i^{th} CC by

$$G_{r|2i} = \left(\frac{P_{r|2i}}{P_{s|2i}|h_{sr|2i}|^2 + P_{t|2i}|h_{tr|2i}|^2 + W_{2i}N_0} \right)^{\frac{1}{2}}, \tag{5}$$

and then it forwards the scaled version to D. The received signal at D is

$$y_{d|2i} = G_{r|2i} h_{rd|2i} y_{r|2i} + \sqrt{P_{t|2i}} h_{td|2i} z_{2i} + n_{d|2i}. \tag{6}$$

and thus, the received end-to-end instantaneous SINR at D over the i^{th} CC of the 2^{nd} frequency band is then given by

$$\gamma_{2i} = \frac{\gamma_{sr|2i}\gamma_{rd|2i}}{\gamma_{sr|2i} + \gamma_{rd|2i} + 1}, \tag{7}$$

where

$$\gamma_{sr|2i} = \frac{P_{s|2i}|h_{sr|2i}|^2}{P_{t|2i}|h_{tr|2i}|^2 + W_{2i}N_0}, \tag{8}$$

$$\gamma_{rd|2i} = \frac{P_{r|2i}|h_{rd|2i}|^2}{P_{t|2i}|h_{td|2i}|^2 + W_{2i}N_0}. \tag{9}$$

3) Total Achievable Rate: Based on Shannon capacity formula, the achievable transmission rate of the SU when R_r is selected, during the 1^{st} time-slot and over the 1^{st} frequency band can be written as

$$\mathcal{R}_{1|r} = \sum_{i=1}^{N_1} W_{1i} \log_2(1 + \gamma_{1i}), \tag{10}$$

while for the second time-slot it is denoted by $R'_{1|r}$, where γ'_{1i} is used in (10) instead of γ_{1i}. Similarly, the achievable rate over the second band during both time-slots is given by

$$\mathcal{R}_{2|r} = \sum_{i=1}^{N_2} \frac{1}{2} W_{2i} \log_2(1 + \gamma_{2i}). \tag{11}$$

The total achievable rate during two time-slots is given by

$$\mathcal{R}_{tot|r} = \left(\frac{1}{2}\mathcal{R}_{1|r} + \frac{1}{2}\mathcal{R}'_{1|r} \right) + \mathcal{R}_{2|r}. \tag{12}$$

The communication of the SU is summarized in Table II.

III. Primary User Outage Probability Threshold

In the literature, each PU usually sets an interference threshold, which translates into a power threshold for the SU, depending on CSI for the links between PU-SU. Perfect CSI could be obtained through direct feedback from the PU, indirect feedback from a third party, and periodic sensing of pilot signal from the PU [7], at cost of increased overhead/feedback. In order to achieve minimum feedback, in this work each

TABLE I
NOTATION

Variable	Explanation	Variable	Explanation	Variable	Explanation
$l=1,2$	Frequency band index	S, D	SU S/D node	W_{li}	CC bandwidth
$N_l/\mathcal{N}_l$	Number/set of CCs in the l^{th} band	T_{li}, V_{li}	PU transmitter/receiver node	γ_{li}	End-to-end SINR
$(\cdot)_{li}$	Value for the l^{th} band and i^{th} CC	R_r	The r^{th} relay	$\gamma_{jq\|li}$	SINR of path $J \rightarrow Q$
$P_{q\|li}$	Power transmitted by node Q	M	Number of available relays	$\mathcal{R}_{l\|r}$	Rate of l^{th} band selecting the relay R_r
$h_{jq\|li}$	Channel gain of path $J \rightarrow Q$	N_0	AWGN power spectral density	$I_{SU\|li}$	Interference caused by the SU network
$G_{r\|li}$	Amplification factor of relay R_r	x_{li}, z_{li}	SU/PU information symbols	$P_{out(S)\|li}$	PU Outage probability caused by S
$K_{q\|li}$	Power threshold for node Q	$y_{q\|li}$	Received symbol at node Q	$P_{out(R)\|li}$	PU Outage probability caused by R_r
$L_{jq\|li}$	Path loss of path $J \rightarrow Q$	$n_{q,li}$	AWGN noise at node Q	$P^{IF}_{out\|li}$	Interference-free PU outage probability

TABLE II
COMMUNICATION OF THE SU NETWORK

Band	Time-slot 1	Time-slot 2
$l=1$	Nodes: $S \rightarrow D$ Power: $P_{s\|1i}$ over the i^{th} CC Rate: $\mathcal{R}_{1\|r^*}$	Nodes: $S \rightarrow D$ Power: $P'_{s\|1i}$ over the i^{th} CC Rate: $\mathcal{R}'_{1\|r^*}$
$l=2$	Nodes: $S \rightarrow R_r^*$ Power: $P_{s\|2i}$ over the i^{th} CC Rate: $\mathcal{R}_{2\|r^*}$ (spans both time-slots)	Nodes: $R_r^* \rightarrow D$ Power: $P_{r\|2i}$ over the i^{th} CC

PU sets a maximum average probability of outage threshold, while a power threshold is sent via feedback to the SU, which depends on the statistical characteristics of the channels and not their instantaneous value.

From (1), the interference imposed by SU on each PU, in the 1st band and during the first time-slot in the 2nd band, is

$$I_{SU|li} = I_{S \rightarrow V_{li}} = P_{s|li}|h_{sv|li}|^2. \quad (13)$$

Therefore, the PU SINR is

$$\gamma_{PU(S)|li} = \frac{P_{t|li}|h_{tv|li}|^2}{P_{s|li}|h_{sv|li}|^2 + W_{li}N_0}. \quad (14)$$

Similarly to [14, Appendix A], if $R_{0|li}$ is the desired data rate and $\bar{R}_{0|li} = 2^{\frac{R_{0|li}}{W_{li}}} - 1$, the outage probability of the PU is

$$P_{out(S)|li} = 1 - \frac{L_{sv|li}P_{t|li}\exp(-L_{tv|li}\bar{R}_{0|li}W_{li}N_0/P_{t|li})}{L_{sv|li}P_{t|li} + L_{tv|li}P_{s|li}\bar{R}_{0|li}}. \quad (15)$$

Similarly, in the 2nd time-slot and 2nd band, the interference is caused by the relay, while the outage probability is

$$P_{out(R)|2i} = 1 - \frac{L_{rv|2i}P_{t|2i}\exp(-L_{tv|2i}\bar{R}_{0|2i}W_{2i}N_0/P_{t|2i})}{L_{rv|2i}P_{t|2i} + L_{tv|2i}P_{r|2i}\bar{R}_{0|2i}}. \quad (16)$$

For a specific average outage probability threshold $\bar{P}_{out|li}$, it must hold that $\bar{P}_{out|li} > P^{IF}_{out|li}$ in order for the threshold to be satisfied, where $P^{IF}_{out|li}$ is the interference-free outage probability of the PU. Based on the expressions in (15) and (16), the corresponding power thresholds for S and each R_r in each frequency band and each CC are calculated as follows:

$$P_{s|li} \leq \left(\frac{\exp(-\frac{L_{tv|li}\bar{R}_{0|li}W_{li}N_0}{P_{t|li}})}{1-\bar{P}_{out|li}} - 1 \right) \frac{L_{sv|li}P_{t|li}}{L_{tv|li}\bar{R}_{0|li}} = K_{s|li}, \quad (17)$$

$$P_{r|2i} \leq \left(\frac{\exp(-\frac{L_{tv|2i}\bar{R}_{0|2i}W_{2i}N_0}{P_{t|2i}})}{1-\bar{P}_{out|2i}} - 1 \right) \frac{L_{rv|2i}P_{t|2i}}{L_{tv|2i}\bar{R}_{0|2i}} = K_{r|2i}. \quad (18)$$

IV. POWER ALLOCATION AND RELAY SELECTION

Taking into account the power thresholds described in the previous section, the SU's total achievable rate maximization problem can be expressed as

$$\begin{aligned} \max_{\mathcal{P}_s, \mathcal{P}'_s, \mathcal{P}_r} \quad & \mathcal{R}_{tot|r} \\ \text{s.t.} \quad & \text{C1}: 0 \leq P_{s|li} \leq K_{s|li}, \text{C2}: 0 \leq P'_{s|li} \leq K_{s|li}, \\ & \text{C3}: 0 \leq P_{r|li} \leq K_{r|li}, \text{C4}: \sum_{l=1}^{2}\sum_{i=1}^{N_l} P_{s|li} \leq P_{s,max}, \\ & \text{C5}: \sum_{i=1}^{N_1} P'_{s|1i} \leq P_{s,max}, \text{C6}: \sum_{i=1}^{N_2} P_{r|2i} \leq P_{r,max}, \end{aligned} \quad (19)$$

where $\mathcal{P}_s = \{P_{s|li} : i \in \mathcal{N}_{l\in\{1,2\}}\}$, $\mathcal{P}'_s = \{P'_{s|1i} : i \in \mathcal{N}_1\}$, and $\mathcal{P}_r = \{P_{r|2i} : i \in \mathcal{N}_2\}$. In (19), $P_{s,max}$ and $P_{r,max}$ denote the maximum power thresholds, which can be transmitted by S and R_r, respectively, and their values are imposed by regulations or hardware specifications.

Problem (19) can be completely separated into two disjoint problems, since the reallocated power over the low frequency band ($\mathcal{P}'_s$) for the second time-slot is independent of the relay selection and power allocation during the first time-slot. The separate problems can be written as

Problem 1:

$$\begin{aligned} \max_{\mathcal{P}_s, \mathcal{P}_r} \quad & \tfrac{1}{2}R_{1|r} + R_{2|r} \\ \text{s.t.} \quad & \text{C1, C3, C4, C6} \end{aligned} \quad (20)$$

Problem 2:

$$\begin{aligned} \max_{\mathcal{P}'_s} \quad & \tfrac{1}{2}R'_{1|r} \\ \text{s.t.} \quad & \text{C2, C5} \end{aligned} \quad (21)$$

The optimal power allocation of S is calculated for each relay, for the case that this specific relay might be selected, before the actual relay selection. Afterwards, the relay which achieves the highest total rate $\mathcal{R}_{tot|r}$ is selected. However, due to the decomposition of the optimization in Problems 1 and 2, the optimization of the transmission $S \rightarrow D$ during the second time-slot (Problem 2) is independent from the relay selection. Therefore, each relay solves Problem 1, in the case that it might be selected. Then, the selection is reduced to

$$R_r^* = \arg\max_r \mathcal{R}_{tot|r} = \arg\max_r \left(\frac{1}{2}\mathcal{R}_{1|r} + \mathcal{R}_{2|r} \right), \quad (22)$$

while Problem 2 is solved after the relay selection and *only* by the selected relay. Finally, the selected relay sends the optimal power allocation as feedback to the S.

A. Solution of Problem 1

Problem 1 is non-convex and, thus, it cannot be solved with acceptable complexity. Therefore, in order to transform it into a convex problem, we consider the following well-known tight approximation for the end-to-end SINR, especially in the medium and high SINR region, as shown in [15]:

$$\gamma_{2i} \approx \tilde{\gamma}_{2i} = \frac{\gamma_{sr|2i}\gamma_{rd|2i}}{\gamma_{sr|2i}+\gamma_{rd|2i}}, \tag{23}$$

The optimization Problem 1 can now be written as

$$\begin{aligned} \max_{\mathcal{P}_s,\mathcal{P}_r} \quad & \frac{1}{2}\mathcal{R}_{1|r} + \tilde{\mathcal{R}}_{2|r} \\ \textbf{s.t.} \quad & \text{C1, C3, C4, C6} \end{aligned} \tag{24}$$

where $\tilde{\mathcal{R}}_{2|r} = \sum_{i=1}^{N_2} \frac{1}{2} W_{2i} \log_2(1+\tilde{\gamma}_{2i})$. The transformed optimization problem in (24) is jointly concave with respect to the optimization variables, since the Hessian matrix of its objective function is negative semi-definite and the inequality constraints are all convex. Moreover, it satisfies Slater's constraint qualification, and, thus, it can now be optimally and efficiently solved with dual decomposition, since the duality gap between the dual and the primal solution is zero [16]. More importantly, it is guaranteed that its global optimum solution can now be obtained in polynomial time. The Lagrangian for the primal problem (24), which is needed in order to solve (24) via dual-decomposition, is given by

$$\begin{aligned} \mathcal{L}(\lambda_1,\lambda_2,\mathcal{P}_s,\mathcal{P}_r) &= \frac{1}{2}\mathcal{R}_{1|r} + \tilde{\mathcal{R}}_{2|r} \\ &- \lambda_1\left(\sum_{l=1}^{2}\sum_{i=1}^{N_l} P_{s|li} - P_{s,max}\right) - \lambda_2\left(\sum_{i=1}^{N_2} P_{r|2i} - P_{r,max}\right) \end{aligned} \tag{25}$$

where $\lambda_1, \lambda_2 >= 0$ are the Lagrange multipliers (LMs) corresponding to the constraints C4, C6. The constraints C1, C3 will be absorbed into the Karush-Kuhn-Tucker (KKT) conditions. The dual problem is given by

$$\min_{\lambda_1,\lambda_2} \max_{\mathcal{P}_s,\mathcal{P}_r} \mathcal{L}(\lambda_1,\lambda_2,\mathcal{P}_s,\mathcal{P}_r). \tag{26}$$

The dual problem (26) can be iteratively solved in two consecutive layers, namely *Layer 1* and *Layer 2*. In each iteration, the subproblems of power allocation are solved for S and R_r in Layer 1 by using the KKT conditions for a fixed set of LMs, which are then updated in Layer 2. This two-layer approach enables the parallelized solution of the identically structured problems that are described in Layer 1, requiring only knowledge of the updated values of the LMs, which are obtained using the gradient method. The aforementioned strategy, which is known to converge after a reasonable number of iterations [17], reduces considerably the required computational and memory resources.

Layer 1: Applying the KKT conditions, the optimal power allocation at the source and the relay over the i^{th} CC is $P^*_{s|1i} = \left[\hat{P}_{s|1i}\right]_0^{K_{s|1i}}, P^*_{s|2i} = \left[\hat{P}_{s|2i}\right]_0^{K_{s|2i}}, P^*_{r|2i} = \left[\hat{P}_{r|2i}\right]_0^{K_{r|2i}}$, in which

$$\hat{P}_{s|1i} = \frac{|h_{sd|1i}|^2 W_{1i} - 2\lambda_1\left(|h_{td|1i}|^2 P_{t|1i} + N_0 W_{1i}\right)\ln(2)}{2\lambda_1 |h_{sd|1i}|^2 \ln(2)}, \tag{27}$$

$$\begin{aligned} \hat{P}_{s|2i} &= -\frac{\Gamma_{1|2i}}{|h_{sr|2i}|^2} + \frac{1}{\ln(4)} \\ &\times\left(\frac{|h_{rd|2i}|^2 W_{2i}\Gamma_{1|2i}}{|h_{rd|2i}|^2\lambda_1\Gamma_{1|2i} - |h_{sr|2i}|^2\lambda_2\Gamma_{2|2i}} + \sqrt{\Gamma_{3|2i}}\right), \end{aligned} \tag{28}$$

$$\hat{P}_{r|2i} = \sqrt{\frac{\Gamma_{4|2i}}{4\ln(2)}} - \frac{|h_{sr|2i}|^2\hat{P}_{s|2i}\Gamma_{2|2i}(|h_{sr|2i}|^2\hat{P}_{s|2i} + 2\Gamma_{1|2i})}{2|h_{rd|2i}|^2\Gamma_{1|2i}(|h_{sr|2i}|^2\hat{P}_{s|2i} + \Gamma_{1|2i})}, \tag{29}$$

$(\cdot)^*$ denotes the optimal solution, and $[\cdot]_0^x = \min(\max(\cdot,0),x)$. In the above, the values of $\Gamma_{1|2i}$ and $\Gamma_{1|2i}$ are given by

$$\Gamma_{1|2i} = |h_{tr|2i}|^2 P_{t|2i} + N_0 W_{2i}, \tag{30}$$

$$\Gamma_{2|2i} = |h_{td|2i}|^2 P_{t|2i} + N_0 W_{2i}, \tag{31}$$

and $\Gamma_{3|2i}$ and $\Gamma_{4|2i}$ are given in (32) and (33) respectively, at the top of the next page. Interestingly, the provided closed-form solutions reveal that, the power allocation at the S and the relay are interdependent.

Layer 2: Since the dual function is differentiable, the gradient method can be used to update the LMs as follows

$$\lambda_1(t+1) = \left[\lambda_1(t) - \zeta_1(t)\left(P_{s,max} - \sum_{l=1}^{2}\sum_{i=1}^{N_l} P_{s|li}\right)\right]^+ \tag{34}$$

$$\lambda_2(t+1) = \left[\lambda_2(t) - \zeta_2(t)\left(P_{r,max} - \sum_{i=1}^{N_2} P_{r|li}\right)\right]^+ \tag{35}$$

where $[\cdot]^+ = \max(\cdot,0)$, $t \geq 0$ is the iteration index and ζ_1, ζ_2 are positive step sizes. Since the problem in (24) is concave, it is guaranteed that the iteration between the two layers converges to the optimal solution of the primal problem in (24), if the chosen step sizes satisfy the infinite travel condition [16], [17].

B. Solution of Problem 2

Problem 2 can also be solved iteratively, using again a two-layer approach. Its Lagrangian is

$$\mathcal{L}'(\lambda_1,\mathcal{P}'_s) = \frac{1}{2}\mathcal{R}'_{1|r} - \lambda_1\left(\sum_{i=1}^{N_1} P'_{s|1i} - P_{s,max}\right) \tag{36}$$

and, thus, the dual problem can be written as

$$\min_{\lambda_1} \max_{\mathcal{P}'_s} \mathcal{L}'(\lambda_1,\mathcal{P}'_s). \tag{37}$$

In each iteration, the optimal power allocation is be given by $P'^*_{s|1i} = \left[\hat{P}_{s|1i}\right]_0^{K_{s|1i}}$, where $\hat{P}_{s|1i}$ is given by (27) for a fixed LM λ_1, which is updated in Layer 2 by

$$\lambda_1(t+1) = \left[\lambda_1(t) - \zeta_1(t)\left(P_{s,max} - \sum_{i=1}^{N_1} P'_{s|1i}\right)\right]^+. \tag{38}$$

$$\Gamma_{3|2i} = \frac{\lambda_2\Gamma_{2|2i}\Gamma_{1|2i}\left(|h_{rd|2i}|^2|h_{sr|2i}|^2W_{2i} - |h_{sr|2i}|^2\lambda_2\Gamma_{2|2i}\ln(4) + |h_{rd|2i}|^2\lambda_1\Gamma_{1|2i}\ln(4)\right)^2}{|h_{rd|2i}|^2|h_{sr|2i}|^2\lambda_1\left(|h_{sr|2i}|^2\lambda_2\Gamma_{2|2i} - |h_{rd|2i}|^2\lambda_1\Gamma_{1|2i}\right)^2}, \tag{32}$$

$$\Gamma_{4|2i} = \frac{|h_{sr|2i}|^4\hat{P}^2_{s|2i}\Gamma_{2|2i}\left(2|h_{rd|2i}|^2W_{2i}\Gamma_{1|2i}(|h_{sr|2i}|^2\hat{P}_{s|2i} + \Gamma_{1|2i}) + |h_{sr|2i}|^4\lambda_2\hat{P}^2_{s|2i}\Gamma_{2|2i}\ln(2)\right)}{|h_{rd|2i}|^4\lambda_2\Gamma^2_{1|2i}\left(|h_{sr|2i}|^2\hat{P}_{s|2i} + \Gamma_{1|2i}\right)^2}. \tag{33}$$

V. Simulation Results

In this section, we present numerical and simulation results for an SU network which aggregates two CCs in each band. The coordinates of the SU nodes are $S(-5,0)$, $D(5,0)$, while the M available relays are situated on the x-axis, equally spaced between points $(-4,0)$ and $(4,0)$. The coordinates of the PU nodes are $T_{11}(-2,7)$, $V_{11}(2,7)$, $T_{12}(-2,10)$ and $V_{12}(2,10)$ for the low frequency band and $T_{21}(-2,-7)$, $V_{21}(2,-7)$, $T_{22}(-2,-10)$ and $V_{22}(2,-10)$ for the high frequency band. The path loss between any node pair p,q is modeled with the bounded path loss model $L_{pq|li} = 1 + d_{pq}^{\alpha_l}$, where d_{pq} is the distance between nodes and α_l is the path loss exponent for each band, which is assumed as $\alpha_1 = 2$ and $\alpha_2 = 2.5$. We further consider normalized bandwidth $W_{1i} = W_{2i} = W = 1$ Hz, while $P_{s,max} = P_{r,max}$. It is assumed that the PUs transmit with power $\frac{P_{t|li}}{N_0} = 15$ dB. Finally, for the PUs holds that $P^{IF}_{out|li} = 10^{-6}$ and $\bar{P}_{out|li} = 1.1 \times 10^{-6}$.

In Fig. 1, the achievable rate of SU is depicted, for $M = 2,4,6$ available relays and different $P_{s,max}$ values. Two cases are assumed, when one CC or two CCs in each band are aggregated. It is observed that the aggregation of more CCs (four instead of two in total) increases the achievable rate, without increasing the total transmitted power. Since the spectrum is shared with the licensed users and the SU transmits without disturbing the PUs, carrier aggregation offers substantial improvement in performance without the need of increased energy consumption. More specifically, the rate that is achieved when two CCs in each band are aggregated, is more than double with respect to the achieved rate when one CC in each band is aggregated, especially for high signal-to-noise ratio (SNR) values. Another observation from Fig. 1 is that the achievable rate reaches a floor when $P_{s,max}$ increases, since the power transmitted by S is constricted by the thresholds set by the PUs. This means that, although the total available power for transmission at S can be $P_{s,max}$, the actual total transmitted power may be less, since otherwise it will impose unacceptable interference on the PUs. A useful observation is that this floor can be substantially improved by adding more available relays, thus enhancing the performance of the SU network. The gain from adding more relays is more evident, when the number of aggregated CCs is larger, since the links benefiting from the selection are more.

When the number of aggregated CCs per band is two, the power allocation at S is as illustrated in Fig. 2. As a reference, the power thresholds which are set by the PUs

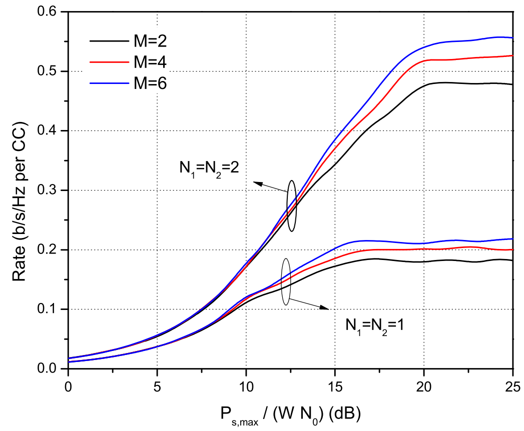

Fig. 1. Achievable rate for $M = 2,4,6$ available relays and for different number of CCs.

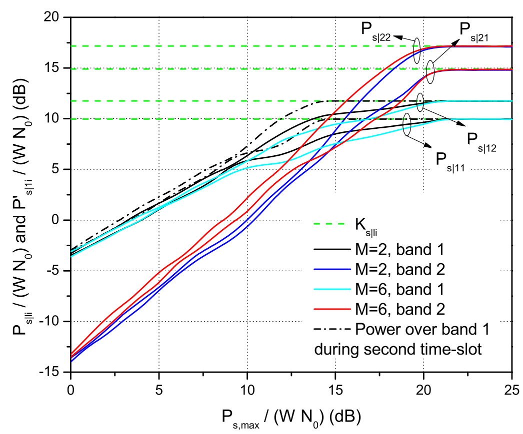

Fig. 2. Power allocation at S for $M = 2,6$ available relays and two CCs per frequency band.

are also illustrated. In the low SNR region, the optimization allocates more power towards D through the direct link, which is preferred due to lower path loss exponent and relative position of the network nodes. However, as the total available power at S increases, the power over the direct link reaches the threshold set by the PUs, and thus more power is sent over the two-hop link. It can be noted that, after the value $\frac{P_{s,max}}{WN_0} = 20$ dB, although there is more power available at S for transmission ($P_{s,max}$), this is not actually transmitted since all CCs have reached the thresholds set by the PUs. In the second time-slot, since S does not transmit over the second band due to the half-duplex operation of the relay, all the available power is transmitted over the first band, where it is optimally divided between the two direct links,until it

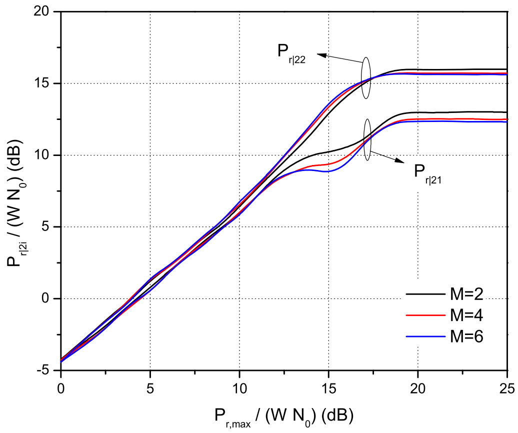

Fig. 3. Power allocation at the selected relay for $M = 2, 4, 6$ available relays and two CCs per frequency band.

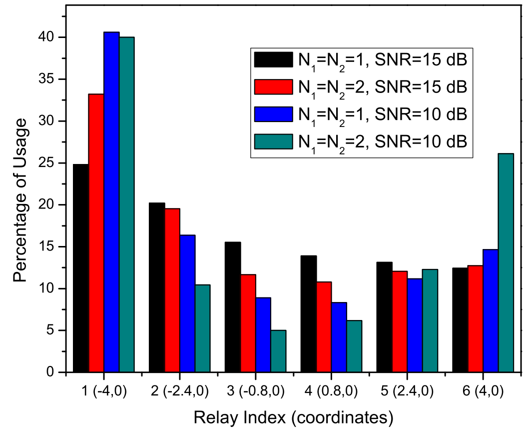

Fig. 4. Relay selection when $M = 6$ relays are available, for SNR=10,15 dB and 1 or 2 CCs per band.

reaches the power thresholds. Furthermore, as the number of available relays increases, the total power which is allocated at the second band increases while the power allocated at the first band decreases accordingly, since there are more choices and thus more available paths. The proposed optimization also allocates the available power at the relay between the two CCs as shown in Fig. 3, for $M = 2, 4, 6$, from which similar conclusions are drawn.

Finally, Fig. 4 presents the percentage of usage of each relay, when $M = 6$ relays are available, for SNR$= 10, 15$ dB, and for one or two CCs per band. The relays are indexed starting from the one closer to S on the x-axis. It is observed that, for all cases, the relay closest to S is most frequently selected. In that case, the noise amplification of the AF protocol is lower. Furthermore, especially for low SNR, the selection tends to select either the first or the sixth relay, because they are situated at a greater distance from the PUs. This is not so evident for high SNR values, since all the relays reach more frequently the power thresholds set by the PUs.

VI. Conclusions

In this paper, we formulated the problem of joint relay selection and optimal power allocation in underlay cognitive radio networks with CA. In the problem formulation we considered multiple CCs and average interference thresholds that are set by the PUs. The non-convex optimization problem was firstly transformed into a convex one and then was solved by using dual decomposition. The simulation results reveal that by applying the proposed method, CA and relay selection jointly offer substantial improvement in throughput.

References

[1] J. Mitola and G. Q. Maguire, "Cognitive Radio: Making Software Radios More Personal," *IEEE Pers. Commun.*, vol. 6, no. 4, pp. 13–18, Aug. 1999.

[2] V. N. Q. Bao, T. Duong, A. Nallanathan, and C. Tellambura, "Effect of Imperfect Channel State Information on the Performance of Cognitive Multihop Relay Networks," in *Proc. 2013 IEEE Global Communications Conference (GLOBECOM)*, Dec. 2013, pp. 3458–3463.

[3] M. Seyfi, S. Muhaidat, and J. Liang, "Relay Selection in Cognitive Radio Networks with Interference Constraints," *IET Communications*, vol. 7, no. 10, pp. 922–930, Jul. 2013.

[4] S. Buljore, H. Harada, S. Filin, P. Houze, K. Tsagkaris, O. Holland, K. Nolte, T. Farnham, and V. Ivanov, "Architecture and Enablers for Optimized Radio Resource Usage in Heterogeneous Wireless Access Networks: The IEEE 1900.4 Working Group," *IEEE Commun. Mag.*, vol. 47, no. 1, pp. 122–129, Jan. 2009.

[5] M. Iwamura, K. Etemad, M.-H. Fong, R. Nory, and R. Love, "Carrier Aggregation Framework in 3GPP LTE-advanced [WiMAX/LTE Update]," *IEEE Commun. Mag.*, vol. 48, no. 8, pp. 60–67, Aug. 2010.

[6] L. Fan, X. Lei, T. Q. Duong, R. Q. Hu, and M. Elkashlan, "Multiuser Cognitive Relay Networks: Joint Impact of Direct and Relay Communications," *IEEE Trans. Wireless Commun.*, vol. 13, no. 9, pp. 5043–5055, Sep. 2014.

[7] Y. Deng, L. Wang, M. Elkashlan, K. J. Kim, and T. Q. Duong, "Generalized Selection Combining for Cognitive Relay Networks Over Nakagami-m Fading," *IEEE Trans. Signal Process.*, vol. 63, no. 8, pp. 1993–2006, Apr. 2015.

[8] D. W. K. Ng and R. Schober, "Resource Allocation and Scheduling in Multi-Cell OFDMA Systems with Decode-and-Forward Relaying," *IEEE Trans. Wireless Commun.*, vol. 10, no. 7, pp. 2246–2258, Jul. 2011.

[9] S. B. Mohamad, C. Y. Leow, and T. A. Rahman, "Relay Placement for Inter-band Carrier Aggregation with Asymmetrical Coverage," in *Proc. IEEE Symposium on Wireless Technology and Applications (ISWTA)*, Sept. 2013, pp. 108–113.

[10] V. N. Q. Bao, T. Q. Duong, D. Benevides da Costa, G. C. Alexandropoulos, and A. Nallanathan, "Cognitive Amplify-and-Forward Relaying with Best Relay Slection in Non-Identical Rayleigh Fading," *IEEE Commun. Lett.*, vol. 17, no. 3, pp. 475–478, Mar. 2013.

[11] L. Li, X. Zhou, H. Xu, G. Y. Li, D. Wang, and A. Soong, "Simplified Relay Selection and Power Allocation in Cooperative Cognitive Radio Systems," *IEEE Trans. Wireless Commun.*, vol. 10, no. 1, pp. 33–36, Jan. 2011.

[12] X. Liu, B. Zheng, and W. Ji, "Cooperative Relay with Power Control in Cognitive Radio Networks," in *Proc. 6th International Conference on Wireless Communications Networking and Mobile Computing (WiCOM)*, Sep. 2010, pp. 1–5.

[13] X. Liu, B. Zheng, J. Cui, and W. Ji, "A New Scheme for Power Allocation in Cognitive Radio Networks Based on Cooperative Relay," in *Proc. 12th IEEE International Conference on Communication Technology (ICCT)*, Nov. 2010, pp. 861–864.

[14] J. Si, Z. Li, and Z. Liu, "Threshold Based Relay Selection Protocol for Wireless Relay Networks with Interference," in *IEEE International Conference on Communications (ICC)*, May 2010, pp. 1–5.

[15] M. O. Hasna and M. S. Alouini, "Performance Analysis of Two-hop Relayed Transmissions over Rayleigh Fading Channels," in *Proc. IEEE 56th Vehicular Technology Conference, (VTC 2002-Fall)*, vol. 4, 2002, pp. 1992–1996.

[16] S. Boyd and L. Vandenberghe, *Convex Optimization*. Cambridge University Press, 2009.

[17] S. Boyd, L. Xiao, and A. Mutapcic, *Subgradient Methods*. lecture notes of EE392o Stanford University Autumn, 2003-2004.